in Proc. SPIE 8091, Biomedical Optics 2011, SPIE/OSA Europe (Munich, Germany, May 22-26, 2011), paper-8091-30.

# Dual excitation waveform Fabry-Pérot tunable filters used in swept sources

I.Trifanov[a], A. Bradu[b], L. Neagu[b], A. Lobo Ribeiro[c] and A. Gh. Podoleanu[b]

[a] Multiwave Photonics S.A., R. Eng. Frederico Ulrich 2650, 4470-605 Moreira da Maia, Portugal
[b]Applied Optics Group, University of Kent, CT2 7NH, United Kingdom
[c] Faculty of Health Sciences, University Fernando Pessoa, R. Carlos da Maia 296, 4200-150 Porto, Portugal.

## ABSTRACT

We report experimental evidence of a novel method to quench the resonances of a Fabry-Perot tunable filter typically used as a wavelength selective element in swept source OCT systems. The method is based on applying a non-sinusoidal, synthesized waveform to the tunable filter, waveform that can be found experimentally in a few iteration steps. A significant improvement in the OCT image quality has been obtained without any software recalibration method.

**Keywords:** swept source, optical coherence tomography, Fabry Pérot tunable filter

## 1. INTRODUCTION

Most wavelength swept laser sources (SS) that use a scanning Fabry–Pérot tunable filter (FP-TF) exhibit nonlinear temporal change of frequency due to the typical sinusoidal excitation waveform applied to the piezoelectric (PZT) element controlling the filter. Ideally, a linear arrangement of data along the k-axis (in wavenumber) is required prior to Fast Fourier Transformation (FFT) in order to yield a correct depth profile. Incorrect optical frequency mapping leads to an A-scan with broadened peaks, that exhibits distortions similar to those due to dispersion left uncompensated in the interferometer. To compensate for the source nonlinearities, a few solutions have been proposed:

a. using a software approach, consisting in resampling the data after analogue-to-digital conversion (A/D) [1];
b. using a hardware approach, consisting in clocking the A/D with an electronic trigger-signal (K-trigger) generated by a second interferometer [2] ;
c. driving the FP-TF with a superposition of sinusoidal waveforms at the first three harmonics of the filter resonance frequencies [3];

These solutions have their own limitations. Thus, the first (software) approach, a, is computationally intensive and reduces the frame rate; the second (hardware) approach, b, is characterized by a higher cost due to the need of a second interferometer and special hardware, including that of a fast digitizer equipped with a specialized clock required to work within a large range of frequencies. Finally, the third approach, c, requires a complex numerical iterative optimization algorithm with 7 variables (amplitudes and phases of the three harmonics and the center wavelength offset) based on a predefined parameter and error maps, and fine experimental adjustments are still needed for final optimization.

Here, we repport a different hardware approach based on generating a synthesized anti-phase modulation waveform function that is applied to the FP-TF. The optimum waveform is found experimentally during an iterative hardware adjustment process. The optimization is simple and rapid, seeking maximum amplitude and minimum width of the FFT peak for a given optical path difference (OPD) value in the OCT interferometer, where the object is replaced with a mirror. Our solution does not require a separate characterization setup, as used by method c.

## 2. EXPERIMENTAL SET-UP AND METHOD

The anatomy of a swept laser source used (SS-OCT) based on a linear cavity fibre configuration with an intra-cavity half symmetrical confocal Fabry-Perot tunable filter is shown in Fig. 1.

The swept laser source [4, 5] is configured as an optical resonator that includes a semiconductor optical amplifier (SOA) as a fast dynamic gain medium (central wavelength 1060 nm, Superlum (County Cork, Ireland)) and a high-speed piezo-electrically driven tuning wavelength element (FP-TF, LambdaQuest (Los Angeles, California)). The filter operates at 1060 nm central wavelength, having a free spectral range FSR ~75 nm and a 0.12 nm line-width. It can be tuned to frequencies up to 40 kHz. The insertion loss of this particular filter is 2.5 dB. A proper optical isolation, by using an optical isolator (ISO) was required before coupling to an external device.

The output of the swept laser is amplified using a PM Ytterbium doped fiber amplifier (YDFA, Multiwave Photonics (Porto, Portugal)) operating in the 1030 - 1080 nm wavelength band, with a 17 dB small signal gain and a saturated output power of 50 mW. The amplified swept laser source spans ~ 50 nm wavelength tuning range and ~45 mW output average power. A saturation build up frequency limit for a ramp waveform applied on the filter has been estimated [3] to be $f_{sweep}$= 27.47 kHz.

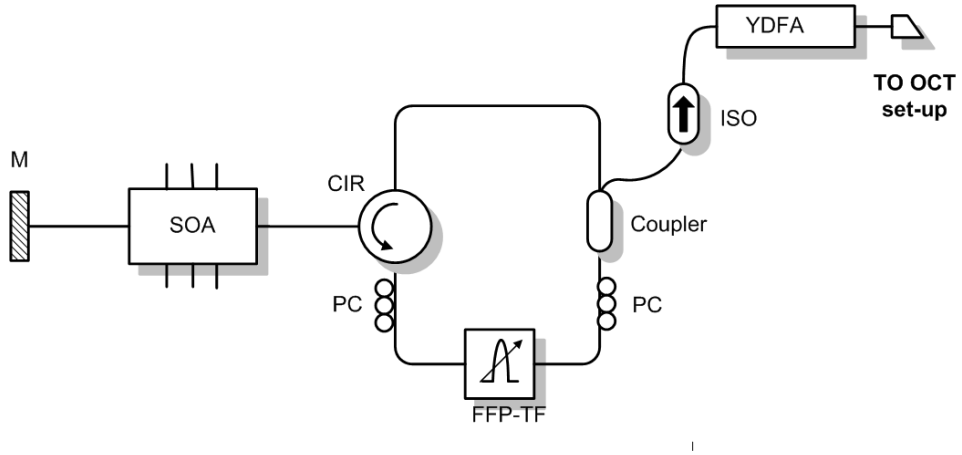


Figure 1. The anatomy of the frequency swept laser-source. SOA: semiconductor optical amplifier, PC: polarization controllers, CIR: optical circulator, FFP-TF: Fabry-Pérot tunable filter, YDFA: ytterbium doped fiber amplifier.

To study the linearity in k-space of such a swept source, its output is coupled to an OCT system designed as a fibre Mach-Zehnder fiber interferometer as shown in Figure 2. Data acquisition is performed using a high speed digitizer card operating at 200 MSamples/s with 12-bit resolution (National Instruments (Austin, Texas), model NI 5124).

The operation of the digitizer was controlled via a LabView$^{TM}$ software program that acquires data synchronously with the voltage applied by the function generator used to tune the FP-TF. Then, it performs a FFT of the acquired signal and displays the interferogram in real time. Both the amplitude of the A-scan as well as the phase variation along the scanned channelled spectrum are displayed.

For a linear excitation of the tunable filter using a ramp or a saw-tooth at slow speed (around 1 kHz), the wavelength generated, $\lambda$ varies linearly in time. In such a regime, a simple software linearization to convert the data to exhibit linear dependence to optical frequency, $\nu$ ($\nu=c/\lambda$, where c is the speed of light) can provide correct A-scan profiles. However, when increasing the excitation frequency, the shorter time required for changing the slope of variation from one ramp to the next becomes closer to the inverse of the mechanical resonance of the FP-TF. Consequently, the higher the frequencies of the applied signal, the larger the deviation of the mechanical response of the FP-TF from the applied drive waveform. This determines a profound nonlinear frequency response of the filter that renders the software linearization inefficient. This phenomenon limits the maximum frequency of the signal applied to the FP-TF.

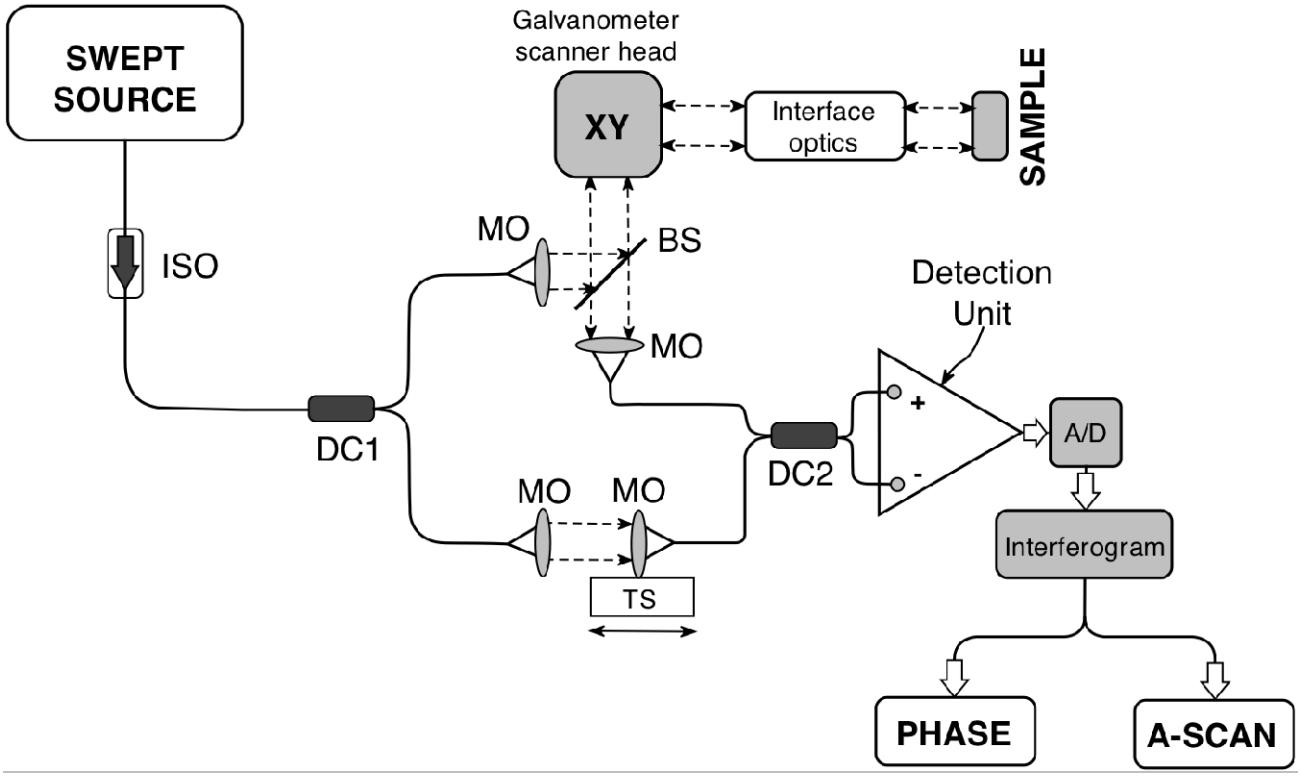


Figure 2**.** Schematic of the OCT set-up configured as a Mach-Zehnder interferometer using directional fibre couplers (DC1,2). Part of the radiation from the source is sent via a bulk beamsplitter (BS), to the interferometer sample-arm, comprising of a pair of orthogonal galvo-scanners and interface optics for imaging. The backscattered signal from the sample is coherently recombined with the interferometer reference-arm at the detector and the optical path difference (OPD) is adjusted using a translation stage (TS). Proper optical isolation (ISO) is required before coupling the source to an external device.

The non-linear response of the filter, although linearly excited at 5 kHz with a ramp waveform, is clearly visible as shown in Fig. 3 (top row). The modulation of the phase of the interferogram (top middle) is the response of this filter to different harmonics of the saw-tooth applied. Also, the FFT of the interferogram (top right) shows broadening of the signal originating from a plane reflector.

Our method consists in adding a second waveform (Burst generator) to the linear ramp (Main generator). By varying the frequency of the second waveform, we realized that we could excite the resonances of the FP-TF and make the phase even more nonlinear. This suggests that if similar excitation is applied, but in anti-phase, it may reduce the mechanical resonances of the filter and its nonlinearity behavior. The proposed hardware solution is illustrated schematically in Fig. 4. The waveform at the top in Fig. 4 shows the main excitation, which determines the operation conditions of the source in terms of frequency sweep, tuning range and duty cycle. The amplitude and the bias voltage of the 1$^{st}$ waveform applied determine the tuning bandwidth (typically 40 nm in this experiment) and the center wavelength (~1060 nm), respectively. Usually, the bias is adjusted to overlap the tuning frequency range of the filter with that of the gain medium. The frequency of the main waveform gives the frequency sweep of the source or the A-scan acquisition speed of the OCT system. In the example shown in Fig. 3, this was set at 5 kHz with a duty cycle of 50% (triangular waveform). The chosen sweep duration equals half of the cycle duration, which in principle can be doubled to a 10 kHz effective sweep frequency in a 2x buffering scheme.

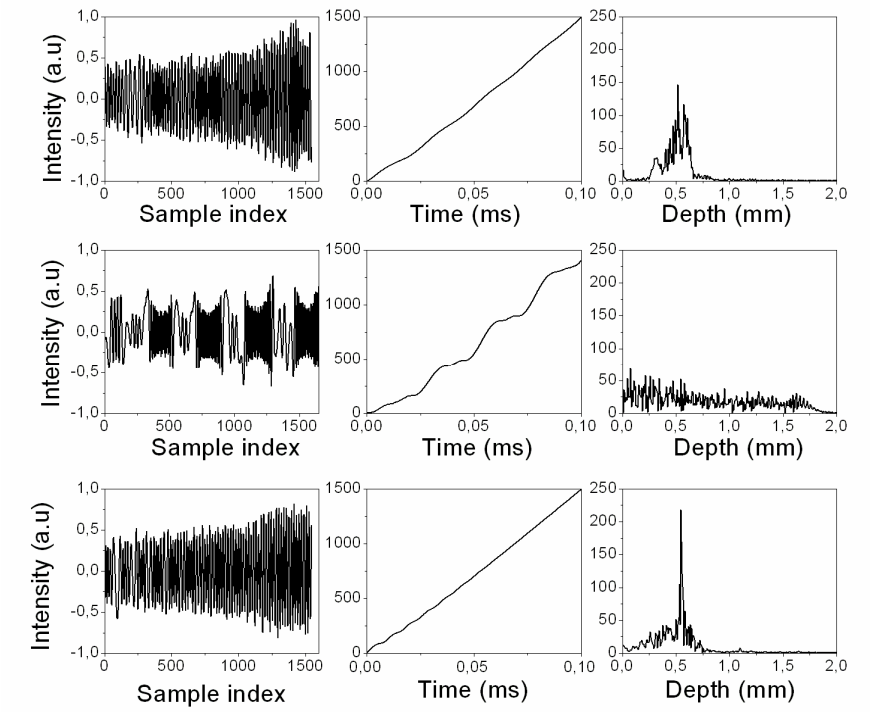


Fig. 3. The interferogram (left), phase (middle) and FFT transform (right) obtained from a mirror object placed in the sample arm of the SS-OCT set-up: Results obtained by using: linear excitation at 5 kHz only (top row); modulation at 50 kHz close to the first resonance of the FP-TF in addition to the linear excitation (middle row); the optimized synthesized shape: 4 burst pulses of sine wave at 101 kHz frequency, with 0.5 $V_{pp}$ amplitude and 28 degree phase superimposed to the linear excitation at 5 kHz (bottom row).

To correct for the nonlinearities of the filter response, a second waveform was applied. This consists in a sequence of pulses in burst mode, generated by a Stanford Research function generator (model DS345). This can be used to generate a number of complete waveform cycles, for each trigger applied, as displayed in Fig. 3 (middle). Burst mode may be used with any arbitrary waveform at any frequency. Full control over the number of pulses, frequency, amplitude and phase is available. The generator is equipped with phase control that allows altering the time of the burst relative to the main waveform by using a trigger synchronized with the main generator. Delay by up to one-half of a period of the burst frequency with respect to an external trigger is possible. The resulting waveform applied to the FP-TF is a quasi-arbitrarily synthesized waveform as displayed in Fig. 4 (bottom). This illustrates an example of the shape of the waveform applied to the FP-TF.

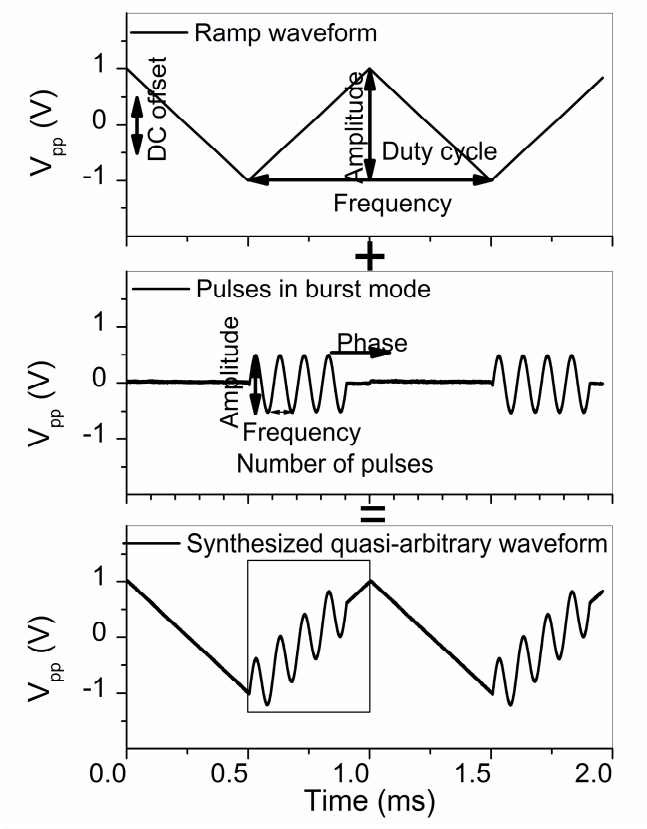


Figure 4. Signal applied to the FP-TF. Top: 1st waveform, linear excitation; Middle: 2nd waveform, burst pulses consisting in 4 sinusoidal cycles; Bottom: synthesized waveform obtained by adding the waveforms above with an adjustable phase difference in between.

By changing the frequency of the modulation applied from the burst generator in steps of 2 kHz at low amplitude (0.5 V and 0 phase), we have been able to identify visually from the interferogram and quantitatively from phase information, FP –TF resonances at approx. 50 kHz, and 100 kHz. Fig. 2 (middle row) displays the response of the filter at the first resonance. Near a resonance, the nonlinearity is exacerbated. This results in an interferogram exhibiting high non-uniformity in fringe spacing (middle row, left), which translates in a high modulation of the phase (middle row, middle) and excessive broadening of the FFT (middle row, right). However, shifting the pulses in time, that is, iteratively increasing the phase values, allows for partially counteracting the effect of the modulation induced by the filter.

## 3. RESULTS

In practice, the parameters of amplitude and phase of the bursts are altered iteratively in order to find the best match that corrects for the nonlinearities of the filter. These are performed while keeping the sinusoidal frequency of the second waveform fixed, close to the first, second or the third resonances of the FP-TF. The adjustment depended critically on the phase and frequency of the bursts and less on the number of cycles in the bursts. Less cycles could be compensated with larger amplitudes to achieve similar effects. However, excessive amplitude applied should be avoided especially when driving the filter near its resonances, because of the electro-mechanical load that may cause overheating and damage.

Fig. 2 (bottom row) shows the results obtained when the optimum quasi-arbitrarily synthesized waveform is applied. A significant improvement is achieved in terms of the width and shape of the A-scan. The optimum parameters found for correcting the response of the filter when using a linear excitation at 5 kHz (triangular waveform) and 8V amplitude were: 4 burst pulses of sine waves at 101 kHz frequency, with 0.5 $V_{pp}$ amplitude and 28 degree phase. If the sine wave frequency deviated from 101 kHz by more than 5 kHz either side, no correction was obtained, even if other phase values were tested.

A set of B-scan OCT images from a sample made of 13 layers of cello tape of 78 μm thickness (measured in air) is displayed in Fig. 4 to illustrate the efficiency of the method. Lateral scanning was performed by applying 3.5 V to one of the transversal scanners in the OCT sample arm at a frame rate of 11.4 Hz. Fig. 4 left displays considerable distortions in the OCT image caused by nonlinear tuning, when the main excitation at 5 kHz was applied alone. The image in the right shows the result after optimization of the waveform using the parameters mentioned in the text. No calibration step or spectral apodization prior to FFT was performed in either case. The image was presented with no software linearization to prove that the technique can significantly contribute towards quenching the resonances of the filter.

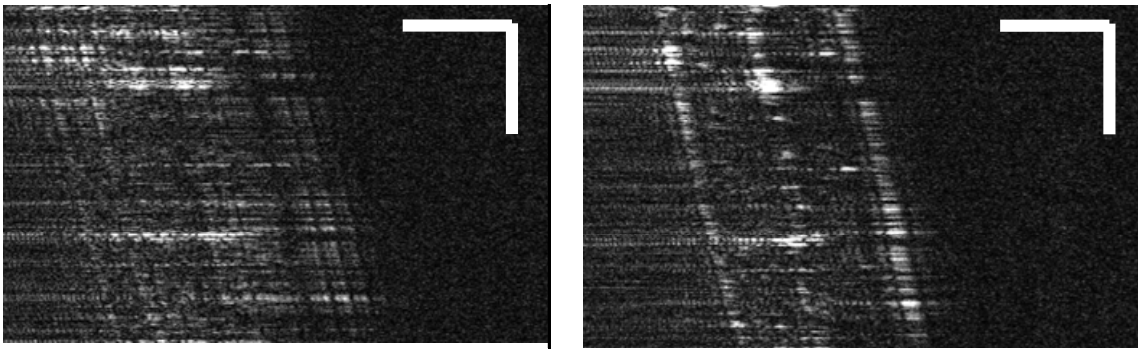

Figure 6. B-scan OCT images obtained using a: linear excitation (top) and the optimum synthesized shape (bottom). Scale bars represent 1 mm.

## ACKNOWLEDGEMENTS

Irina Trifanov acknowledges the Marie Curie training site grant supported by the European Commission (EC MEST-CT-2005-020353). Adrian Bradu and Adrian Podoleanu acknowledge the support of the European Research Council (http://erc.europa.eu/), grant 249889.

## REFERENCES

1. S. Vergnole, D. Lévesque, and G. Lamouche, "Experimental validation of an optimized signal processing method to handle non-linearity in swept-source optical coherence tomography," *Opt. Express* vol. 18, pp. 10446-10461, 2010.
2. J. Xi, L. Huo, J. Li, and X. Li, "Generic real-time uniform K-space sampling method for high-speed swept-Source optical coherence tomography," *Opt. Express* vol. 18, pp. 9511-9517, 2010.
3. C. M. Eigenwillig, B.R. Biedermann, G.Palte, and R.Huber, "K-space linear Fourier domain mode locked laser and applications for optical coherence tomography," *Opt. Express* vol. 16, pp. 8916-8937, 2008.
4. I. Trifanov, L. Neagu, A. Bradu, A. Gh. Podoleanu and A.B. Lobo Ribeiro, "Characterization of a swept source at 1 μm for optical coherence tomography", in Proc. SPIE vol.7889, paper 7889-100, 2011.
5. R. Huber, M. Wojtkowski, K. Taira, J. Fujimoto, and K. Hsu, "Amplified, frequency swept lasers for frequency domain reflectometry and OCT imaging: design and scaling principles," *Opt. Express* vol. 13, pp. 3513–3528, 2005.